Morphology of Gas-Assisted and Conventional Injection Molded Polycarbonate/Polyethylene Blend

Guoqiang Zheng,[1] Wei Yang,[1] Bo Yin,[1] Mingbo Yang,[1] Chuntai Liu,[2] Changyu Shen[2]

[1]*College of Polymer Science and Engineering, State Key Laboratory of Polymer Materials Engineering, Sichuan University, Chengdu, Sichuan 610065, People's Republic of China*
[2]*National Engineer Research Center for Advanced Polymer Processing Technology, Zhengzhou University, Zhengzhou, Henan 450002, People's Republic of China*

Received 3 November 2005; accepted 8 February 2006
DOI 10.1002/app.24792
Published online in Wiley InterScience (www.interscience.wiley.com).

ABSTRACT: The skin-core structure of the gas-assisted and conventional injection molded polycarbonate (PC)/polyethylene (PE) blend was investigated. The results indicated that both the size and the shape of the dispersed PC phase depended not only on the nature of PC/PE blend and molding parameters, but also on its location in the parts. Although the gas-assisted injection molding (GAIM) parts and conventional injection molding (CIM) part have the similar skin-core structure, the morphology evolution of PC phase in the GAIM moldings and the CIM moldings showed completely different characteristics. In the section perpendicular to the melt flow direction, the morphology of the GAIM moldings included five layers, skin intermediate layer, subskin, core layer, core intermediate layer as well as gas channel intermediate layer, according to the degree of deformation. PC phase changed severely in the core layer of GAIM moldings, as well as in the subskin of CIM moldings. In GAIM parts, PC phase in the core layer of the nongate end changed far more intensely and aligned much orderly than that in the gate end. The morphology of PC phase in the GAIM part molded with higher gas pressure changed more severe than that in the GAIM part molded with lower gas pressure. In a word, PC phase showed more obvious fibrillation in the GAIM moldings than that in the CIM moldings. © 2006 Wiley Periodicals, Inc. J Appl Polym Sci 102: 3069–3077, 2006

Key words: PC/PE blend; gas-assisted injection molding; conventional injection molding; morphology; shear rate

INTRODUCTION

Gas-assisted injection molding (GAIM), an innovative molding process,[1,2] has been recently developed on the basis of conventional injection molding (CIM), and a schematic diagram of GAIM is shown in Figure 1. Generally speaking, GAIM basically includes three stages: (1) the melt is partly injected into mold cavity, namely the short-shot; (2) after the delay time, high-pressure gas is injected into the melt, which propels the melt forward until it reaches the end of the mold cavity; (3) gas continues to pressurize the melt to cling to the mold wall until the melt is solidified. Compared with CIM, GAIM has many advantages,[1–14] such as substantially reducing material cost, clamping tonnage, cycle time, and prolonging the life-span of injection machine. In addition, some defects encountered in CIM, such as residual stresses, warpage, and sink marks, can be substantially eliminated, especially for the large parts whose quality and rigidity are the main concerns when employing GAIM.

Researchers have paid much attention to GAIM, in view of its intrinsic advantages. So far, most literatures mainly focused on the mathematic simulation of gas penetration,[4–8,11–15] the effect of the gas channel design on the gas penetration behavior,[3,4,6,16] molding window,[3,10,17] the influence of gas channel shape on the mechanical properties[18–20] and so on, while studies on the morphology development in GAIM part and the relationship between microstructure and macroproperties are limited. Chien[21] explored the influence of gas channel shape on the mechanical properties of GAIM moldings as well as the crystallnity of polyamide (PA), and found that maximum tensile load and ultimate tensile stress of PA moldings exhibited significant dependence on part thickness because of higher degree of crystallinity. Liu et al.[22] investigated the fiber orientation in the water-assisted injection molded polypropylene (PP), which was filled with glass fiber, and found that fibers highly oriented in the mold/polymer interface and the polymer/water interface rather than in the center of the thickness.

The morphological anisotropy characteristic of conventional injection-molded blends is primarily the result of orientation of phases along the complex melt flow lines during mold filling,[23–27] which include the

Correspondence to: M. Yang (yangmb@scu.edu.cn).
Contract grant sponsor: National Nature Science Found of China; contract grant number: 10590351.
Contract grant sponsor: the Major State Basic Research Projects; contract grant number: 2005CB623808.

Journal of Applied Polymer Science, Vol. 102, 3069–3077 (2006)

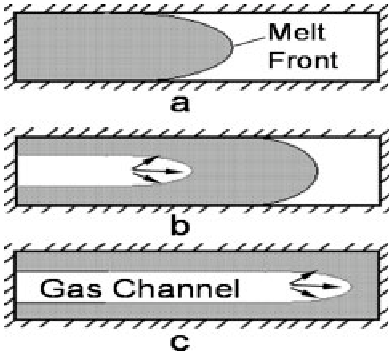

Figure 1 Schematic diagram of GAIM process: (a) partial melt filling; (b) gas-assisted filling; (c) gas-assisted packing.

''fountain flow'' pattern at the melt front. Previous studies[27–29] showed that blends molded by CIM generally present skin-core structure. Recently, Fellahi and coworkers[30] studied the morphology of the high-density polyethylene/polyamide–6 blend molded by CIM, and SEM results showed that the dispersed phase PA6 oriented greatly in the subskin and exhibited spherical particles in the core region. Son and coworkers[31] reported that across the part thickness, poly (phenylene oxide)/polyamide–6 blends molded by CIM comprised distinct skin, subskin, and core region. The position of the subskin was mainly determined by the injection flow rate and the aspect ratio of the dispersed phase chiefly depended on the melt temperature. Detailed morphology study of PC/PE blend molded by CIM was carried out by Li and coworkers.[32] SEM micrographs showed that the section perpendicular to the melt flow direction included four layers (surface, subskin, intermediate layers as well as core zone) according to the shape and the size of dispersed phase. PC phase was in the fibrillar form in subskin for the larger shear rate it experienced.

However, the morphology and the morphology-properties relationship of GAIM molded parts were very limited, and great effort is needed urgently. The objective of this study is to investigate the morphological difference induced by the gas-assisted and conventional injection molded immiscible blend, namely PC/PE, using a mold depicted in Figure 2.

EXPERIMENTAL

Materials

The resins used in this study were PC and HDPE, whose nature properties can be found elsewhere.[32]

Preparation of samples

PC was dried under vacuum at 100°C for at least 10 h to get rid of the moisture before dry-mixing with HDPE with a fixed weight ratio of 20/80. The mixture was then blended in a TSSJ-25 twin-screw extruder with a temperature profile of 150, 190, 230, 265, 275, and 270°C from hopper to die. The rotation speed of the screw was maintained at 120 rpm. The extrudate in the form of thread extruded through a rod die was palletized and dried before molding.

A Grand 140–320 injection molding machine and a MPC model gas injection system with the capacity of five-stage pressure profile control (one stage of gas injection was used) were used for the molding process. The processing parameters of gas-assisted and conventional injection molding were listed in Table I. According to the gas pressure settled in GAIM, the samples obtained from GAIM was divided into two groups, lower gas pressure and higher gas pressure. The cross sections' photographs of the GAIM moldings at A, B (see Fig. 2) and the middle of them were showed in Figure 3, where the left was taken from A and the right from B. It is clear that gas channel diameter of A (close to the gate end) is larger than that of B (close to the non-gate end).

Scanning electron microscopic observation

To get the surfaces for scanning electron microscope (SEM) observation, first, specimens were cut from the shadow labeled A and B (see Fig. 2) in the parts molded by GAIM and CIM as well. Then the specimens and the PC/PE blend thread extruded were put into liquid nitrogen for about 40 min. At last, the specimens were broken along the flow direction to make surfaces for SEM observation (shown in Fig. 4). Before observation, the specimens were gilded in a vacuum chamber to make them conductive. The phase morphology was observed in a SEM instrument, JSM-5900LV, operating at 20 kV.

RESULTS

Original morphology of PC/PE blend

Typical morphology of the PC/PE blends after extrusion was shown in Figure 5. It was obvious that PC phase exhibited spherical and ellipsoidal shape, indicating that the shape of PC phase changed slightly in the extrusion process. Some of the PC particles adhered

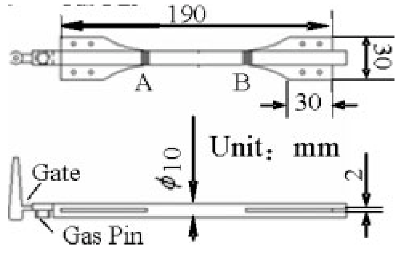

Figure 2 Geometry of the GAIM part.

TABLE I
The Molding Parameters Used

Parameters	GAIM: Higher gas pressure	GAIM: Lower gas pressure	CIM
Injection pressure (MPa)	80	80	80
Gas packing pressure (MPa)	8.274	19.396	–
Packing pressure (MPa)	–	–	60
Delay time (s)	1	1	–
Gas packing time (s)	10	10	–
Cool time (s)	60	60	60
Melt temperature (°C)	280	280	280
Mold temperature (°C)	30	30	30
Short-shot size (Vol %)	85	85	–

to the surface of the PE matrix and the others fell down during sampling, leaving many grooves in the matrix. The interfaces between PC and PE were very smooth and there was not any evidence of adhesion, indicating that the two resins were severely incompatible. The diameter of the PC particles was in a range of distribution, and its mean diameter was 0.8 μm.

Comprehensive inquisition of the morphology in the GAIM moldings

According to the degree of deformation, the morphology of the GAIM moldings included five layers (skin intermediate layer, subskin, core layer, core intermediate layer, and gas channel intermediate layer) perpendicular to the melt flow direction. SEM micrographs of PC/PE blend molded by GAIM in the regions parallel to the melt flow direction were presented in Figures 6 and 7. The pictures labeled a–e, and a′–e′ were obtained from the mold/polymer interface to the polymer/gas channel interface. For short, the mold wall/polymer interface was called skin layer, and the polymer/gas channel gas channel layer. The skin and gas channel layer were neglected in this study because there was no PC phase in them.

At the gate end, spherical and ellipsoidal forms of PC/PE blend molded at lower gas pressure in the skin intermediate layer transformed into irregularly club-shaped and fibrillar forms in the subskin, while ellipsoidal and irregularly club-shaped forms of PC/PE blends molded at higher gas pressure in the skin intermediate layer transformed into fibrillar form in the subskin. In the core layers, PC phase exhibited fibrous form in specimens molded at both lower and higher gas pressure. For both parts molded at lower and higher gas pressure, the core intermediate layers consisted of many elongated particles and more or less club-shaped bars with different degree of deformation, whereas PC phase exhibited well-defined particles and elongated bars in the gas channel intermediate layer.

At the nongate end, PC phase was in the form of ellipse, sphere, and bar in the skin intermediate layer of the both specimens molded at lower and higher gas pressure. More fibers with a larger degree deformation appeared in the subskin. As for the parts molded at lower and higher gas pressure, PC phase in the core layer exhibited fibrillar form and extreme orientation. The core intermediate layers were transition regions where less particles, more bars, and fibers coexisted. PC phase was in elongated form with a smaller degree

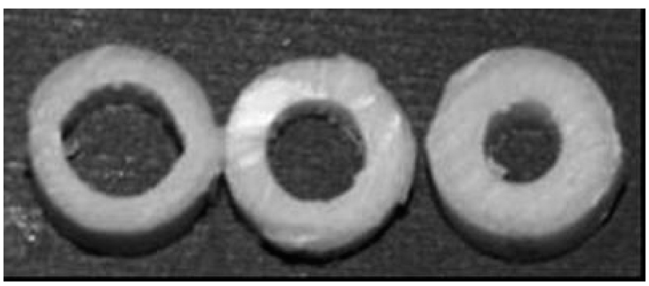

Figure 3 The cross sections from the gate (the left) to the nongate.

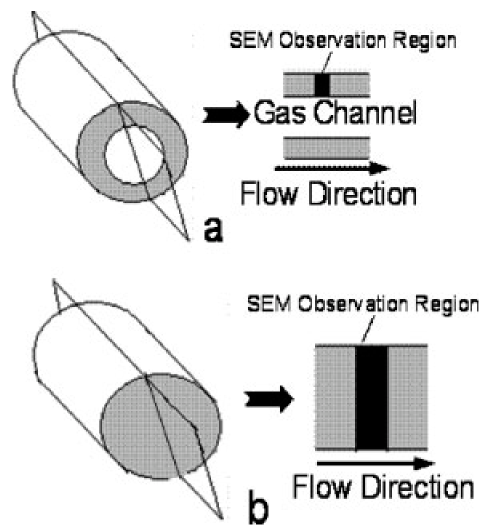

Figure 4 Regions for SEM observation of GAIM (a) and CIM (b).

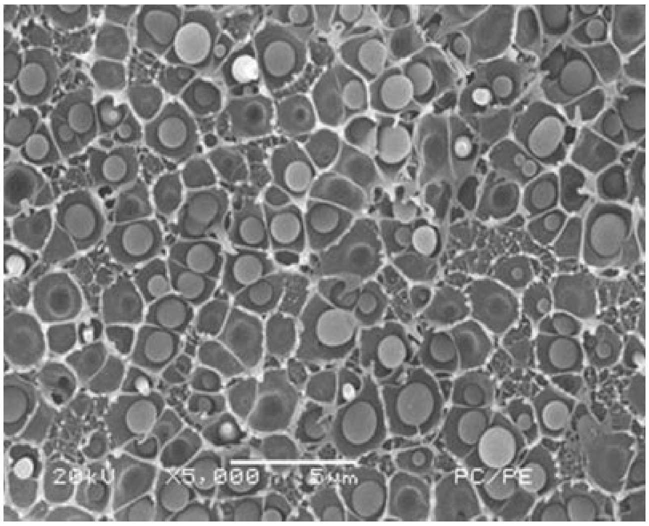

Figure 5 Typical morphology of the PC PE blend after extrusion.

of deformation in the gas channel intermediate layer. Following conclusions could be drawn by comparing the micrographs in Figure 6 and Figure 7.

1. For both specimens molded at lower and higher gas pressure, PC phase at the gate end was of a greater degree deformation in the subskin layer and the core layer than that in the skin intermediate layer, core intermediate layer and gas channel intermediate layer. At the nongate end, PC fibers in the core layer had smaller diameter and aligned more orderly than that in the core layer at the gate end. The morphology at the nongate end was of a greater degree deformation than that at the gate end.
2. At the nongate end, the diameter of the fibers, especially in the core layer of the part, molded at higher gas pressure was much smaller than that molded at lower gas pressure, which indicated that higher gas pressure had a more powerful fibrillation effect than the lower did.
3. At the gate end, the specimen molded at higher gas pressure had no obvious difference in morphology from that molded at lower gas pressure in the same layer, which indicated that gas pressure influenced the morphology slightly in this region.
4. For the parts molded at the same gas pressure, the thickness of the core layer (the distance from the subskin to the core intermediate layer) at the gate end is much more thicker than that at the nongate end. For example, the thickness of the core layer at the gate end and the nongate molded at lower gas pressure was respectively, 0.128 mm and 0.236 mm, while that at the gate end and the nongate end molded at higher gas pressure was respectively, 0.276 mm and 0.517 mm.

Full investigation of the morphology of the CIM moldings

According to the degree of deformation, the morphology of the conventional injection molded parts included four layers, skin intermediate layer, subskin, core intermediate layer, as well as core layer perpendicular to the melt flow direction. SEM micrographs of the PC/PE blend molded by CIM over the cross section at A (at the gate end) and B (at the nongate end) in the melt flow direction were presented in Figure 8. It could be noticed that PC phase was primarily of the club-shaped form in the skin intermediate layer at the gate end, while spheres and elongated spheres dominated in the same region at the nongate end with only a few PC particles in the rod-like form. In the subskin, PC phase were of fibrillar form with larger diameter at the gate end. In contrast, much more PC particles were rod-like in the subskin at the nongate end. At the gate end, the core intermediate layer was a transition zone, where PC bars with large diameter, elliptical particles and spheres coexisted, while more elongated particles exhibited in the same layer at the nongate end. Not only at the gate end but also at the nongate end, PC phase was primarily of spherical and elongated forms in the core layer. Comparing the morphology of the same layers at the gate end and the nongate end, the following results could be obtained:

1. In the same layer, PC phase at the gate end was deformed to a larger degree than that at the nongate end, which indicated that PC particles experienced much fiercer elongation at the gate end.
2. PC fibers at the gate end ranked more orderly than that at the nongate end.
3. The thickness of the subskin, in which PC phase had the largest deformation, reduced from the gate end to the nongate end. For example, at the gate end, it was 0.358 mm in contrast with the 0.221 mm at the nongate end.

Morphology comparison between the GAIM and CIM moldings

Though all the specimens molded by both GAIM and CIM exhibited typical skin-core structure as reported in the previous literatures[27–29,32], there was obvious morphological difference between the specimens molded by the earlier-mentioned two processing means. The following results were obtained by comparing the morphology in Figures 6–8:

1. At the gate end of the CIM moldings, PC fibers in the subskin oriented much more intensely than that in the core layer of the GAIM moldings. At the nongate end, PC fibers in the core layer of the GAIM moldings were of much smaller diameter

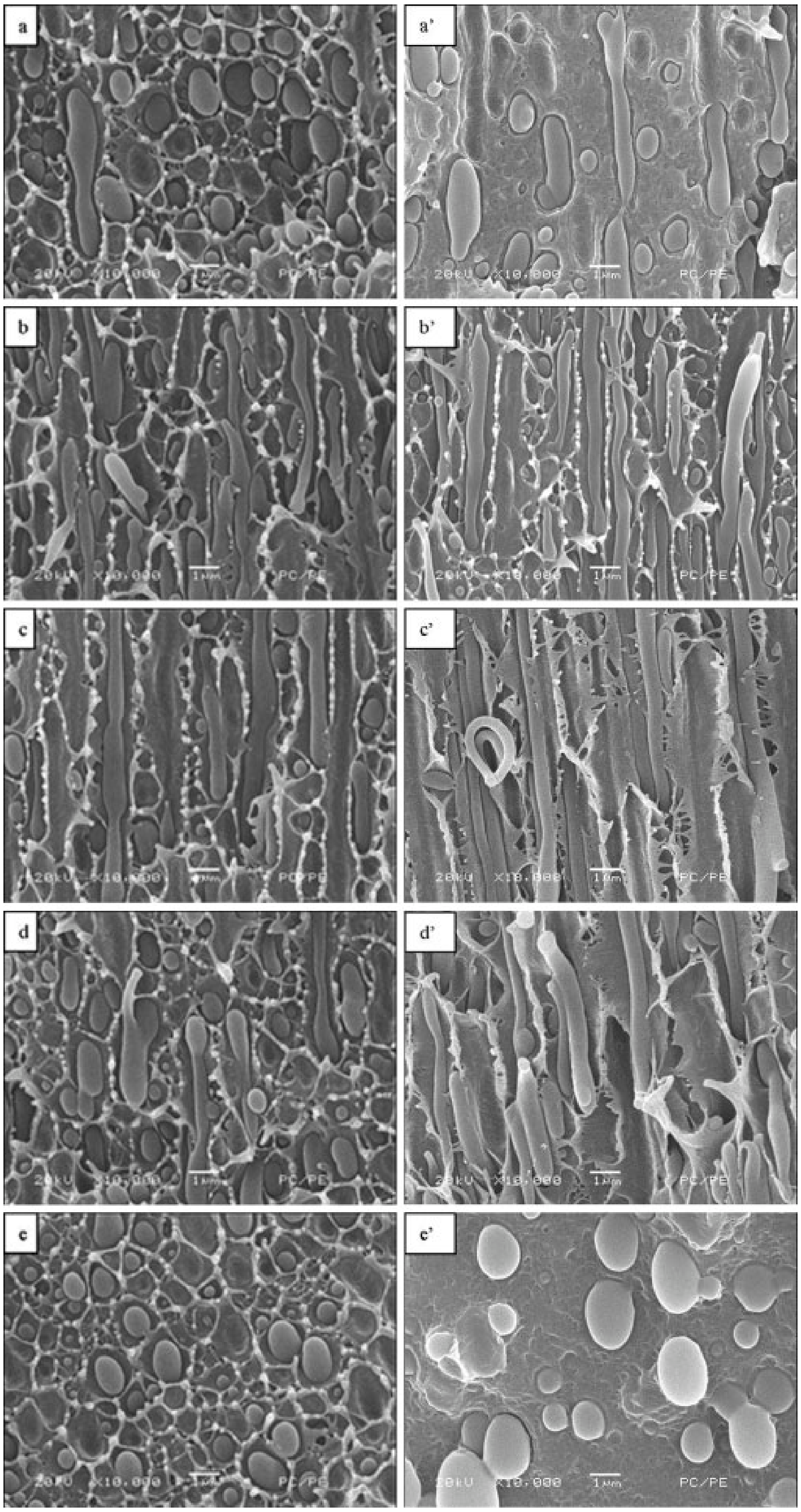

Figure 6 SEM micrographs at different positions of A and B of the GAIM part molded at lower gas pressure (8.274 MPa): (a,a′) skin intermediate layer; (b,b′) subskin; (c,c′) core; (d,d′) core-intermediate layer; (e,e′) gas-channel intermediate layer. a, b, c, d, and e represent region A (close to the gate end); a′, b′, c′, d′, and e′ represent region B (close to the nongate end).

and ranked much more orderly than that in the subskin of the CIM moldings.

2. Generally speaking, at the gate end, compared with the morphology in the skin intermediate layer and the subskin of the CIM moldings, the morphology in the same layers of the GAIM moldings was of much smaller deformation. However the PC phase at the nongate end in

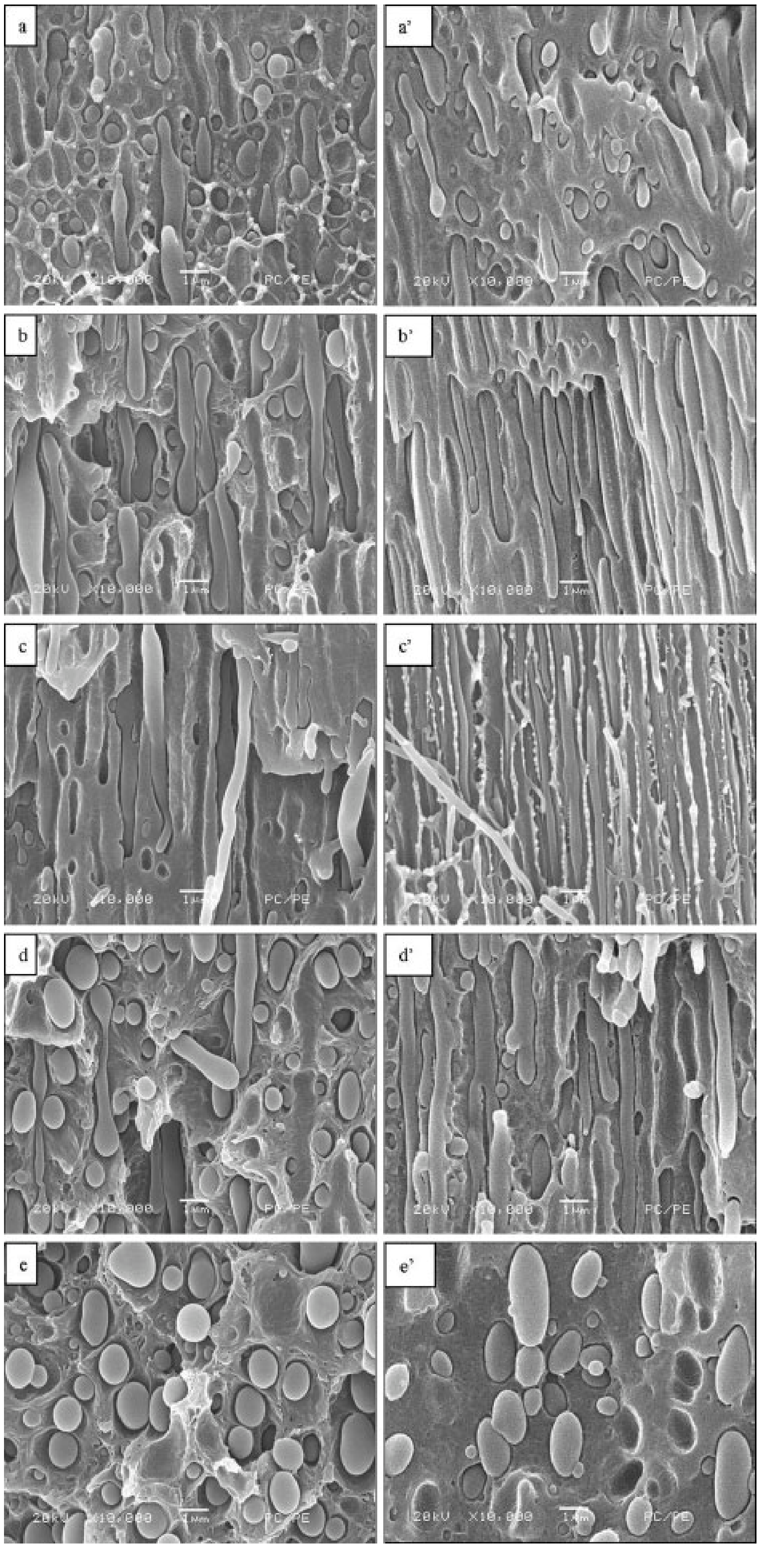

Figure 7 SEM micrographs at different positions of A and B of the GAIM part molded at higher gas pressure (19.396 MPa): (a,a′) skin intermediate layer; (b,b′) subskin; (c,c′) core layer; (d,d′) core intermediate layer; (e,e′) gas-channel intermediate layer. a, b, c, d, and e represent region A (close to the gate end); a′, b′, c′, d′, and e′ represent region B (close to the nongate end).

the GAIM moldings was deformed to larger degree than that at the gate end in CIM part.

3. On the whole, the morphology at the gate end of the GAIM parts was of smaller deformation than that at the nongate end, whereas the morphology at the gate end of the CIM parts was of greater deformation than that at the nongate end.

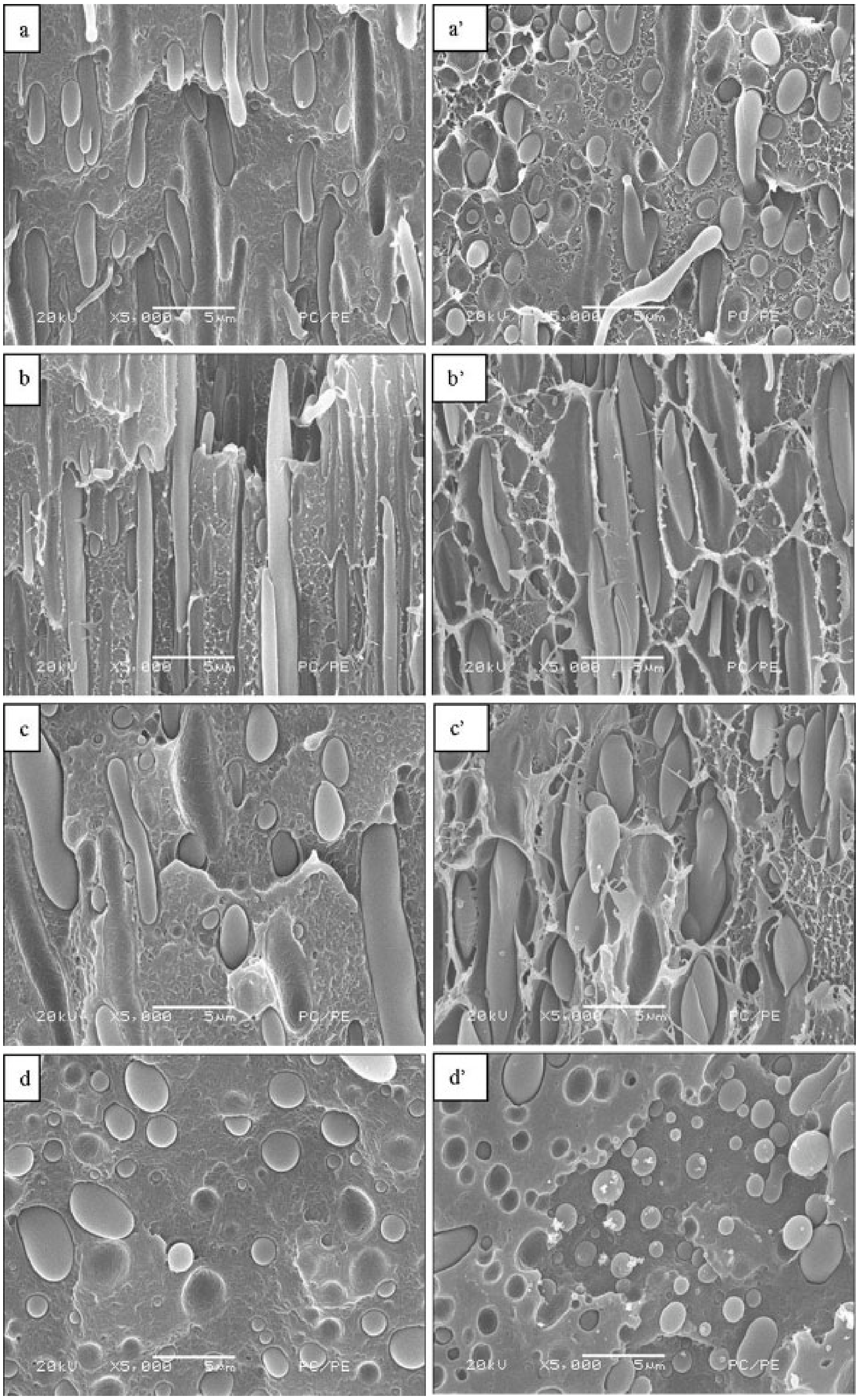

Figure 8 SEM micrographs of the PC PE blends at different positions molded by conventional injection molding: (a,a′) skin intermediate zone; (b,b′) subskin; (c,c′) core intermediate zone; (d,d′) core; a, b, c, and d represent region A (close to the gate end); a′, b′, c′, and d′ region B (close to the nongate end).

DISCUSSION

Because a single-gate mold was used in this study, the polymer melt filled the cavity successively in the pattern of ''fountain flow'' from the gate to the nongate end in the CIM process. GAIM involves in two major filling stages, namely partial melt filling and gas-assisted filling (see Fig. 1). Therefore the morphology transition from the gate to the nongate end should not be continuous. As a result, to characterize the overall morphology development along the flow direction, the morphology between the gate and nongate end should be carefully speculated. In the GAIM process, the morphology development over the entire section in the melt flow direction could be schematically illustrated in Figure 9 on the basis of the earlier-mentioned morphology description. Like that in the CIM part, the PC phase exhibited the greatest deformation at the gate end of the GAIM moldings and appeared in the region close to the mold wall. At the nongate end, the core layer was broadened and deviated from the region closing the mold wall to the center of the part thickness. The origin of the morphology development for PC/PE blend molded by CIM process had been illuminated previously,[32] so just the different mechanism of the PC phase deformation between the GAIM process and CIM process was paid attention to in this paper.

As discussed earlier, the PC phase was chiefly in the spherical and ellipsoidal forms since it underwent a small degree of deformation during the blending. The final morphology of the dispersed phase in the GAIM moldings depended on the flow fields exerted by the melt and gas during mold filling, and the cooling rate during and after molding filling. Dispersed phase could be deformed, broke up, and coalesced in the shear and elongational fields. So the final microstructure of the parts was the mutual outcome of the factors mentioned already.

In view of the different cooling rate, in the short-shot step of GAIM, a frozen layer (namely skin) would come into being once the melt touched the cavity wall. However, the melt in the center of the cavity kept on advancing until the melt filing ended, due to the propelling of the melt followed. Therefore, the maximum shear rate appeared in the region between the skin and

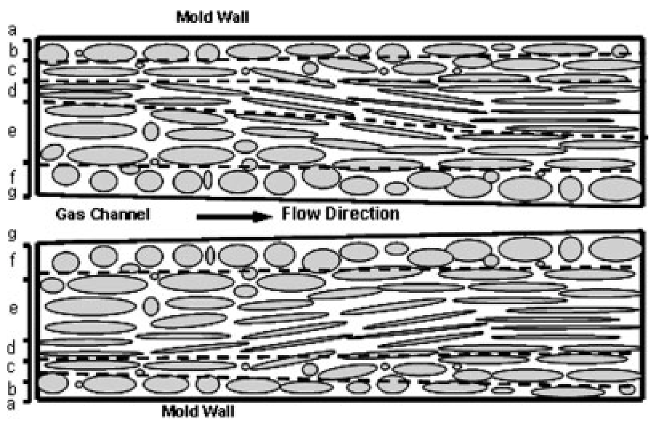

Figure 9 The schematic model of the morphology development in GAIM part along the melt flow direction: (a) skin; (b) skin intermediate layer; (c) subskin; (d) core layer; (e) core intermediate layer; (f) gas-channel intermediate layer; (g) gas-channel layer.

the melt in the center of the mold cavity, which was still going forwards, while the shear rate was zero in the core of the melt.[33] As a result, the PC phase deformed severely in the region closing the mold wall because of the maximum shear effect experienced. Such a process is similar to that in CIM process. The pressure inside the melt at the gate end was very low during the cession of the short shot and the beginning of gas-assisted filling (see Fig. 1). In return, lower interfacial contact occurred between the dispersed phase and the matrix. Because of the lower interfacial contact, PC phase that had been deformed during the short shot would recover during the delay time. This could explain why the PC phase at the gate end of the CIM part deformed much more seriously and ranked much orderly than that in the GAIM moldings. Why did not the PC particles in the melt propelled by the high-pressure gas deform and orient extremely in the gas channel intermediate layer? The reason should be that the gas used in this experiment was of much smaller viscous coefficient,[34] especially under supercritical condition[35] during the gas-assisted filling. Hence, there is almost no friction between the gas channel layer and the supercritical gas. Consequently, the supercritical gas close to the edge of the channel will not draw the adjacent melt to flow with it. Thus, the PC particles in the gas channel intermediate layer phase would not present fibrillation and orientation induced by the high-pressure gas. On the whole, the shape and the size change of PC phase at the gate end of GAIM moldings was the balance of the elongation and the recovery, with the former brought out by the higher shear during the melt filling and the latter came about before the beginning of the gas-assisted filling, and the deformation of PC phase at the gate end had nothing to do with the pressure of the nitrogen gas used in this study.

Additionally, there was temperature difference between the supercritical nitrogen and the melt because the gas was at room temperature. Thus, the gas in the gas channel would cool the melt close to the gas channel layer when the high-pressure gas pushed the melt front forward. So the viscosity of the melt close to the gas channel layer would become higher. In the light of viscosity, the overall fracture surface between the mold wall and the gas channel consisted of three layers: the layer close to the mold wall with the highest viscosity, the layer close to the gas channel with a higher viscosity, and the core layer with a lower viscosity. Since the gas front is enveloped by melt, at the nongate end, the high-pressure gas not only penetrated the melt but also pushed the melt layer, closing the gas channel forward during the gas-assisted filling (see Fig. 1). However, the melt in the melt front would cease flowing once it touched the mold wall. In return, there was velocity difference between the skin and the gas-channel layer. Consequently, relative motion occurred between the melt closing the gas channel and that closing the mold

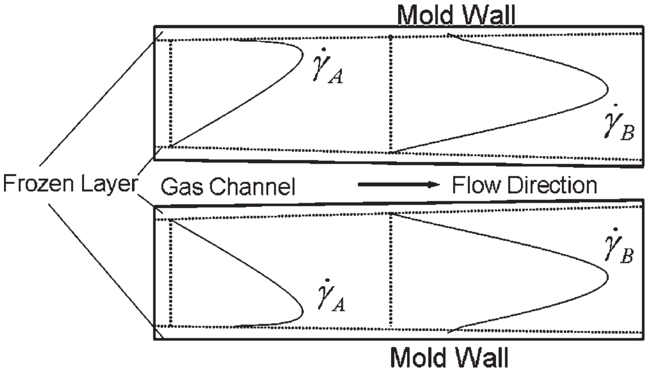

Figure 10 Shear rate profile of the gas-assisted molded part along the flow direction during mold filling.

wall. Thus, the PC phase in the core layer deformed extremely and aligned orderly because of the relative motion between the sun-skin and the gas channel layer, and the thickness of the core layer (the distance between the subskin intermediate layer and the gas channel intermediate layer) at the nongate end was larger than that at the gate end as well. On the basis of above discussions, the shear rate profile at the gate end and the nongate end was depicted in Figure 10, which presents much difference from the shear rate profiles proposed in the literatures.[32,36] The shear rate reached its maximum at the nongate end, and the maximum shear rate at the nongate end appeared in the region approaching the center of the thickness of the part, whereas the maximum shear rate at the gate end was in the region closing the mold wall.

CONCLUSIONS

In this paper, the morphology evolution of the GAIM and CIM moldings was investigated, and the following conclusions could be drawn:

1. The natural properties of PC/PE blend, molding parameters (such as gas pressure), the positions in the molded part etc. were the main factors that determined the shape and the size of the PC phase.
2. In this experiment, the morphology of the GAIM moldings were found to be more complex in the section perpendicular to the melt flow direction and consisted of more layers than that in the CIM parts.
3. At the gate end, the deformation of PC phase in both GAIM and CIM moldings was basically of the same mechanism, because melt flow was the leading inducement for the deformation of PC phase.
4. The origin of the morphology development at the nongate end of the GAIM part was different from that at the gate end. The maximum shear rate deviated from the subskin at the gate end to the core layer at the nongate end, which was ascribed to the high-pressure gas penetration in the melt.
5. The PC particles at the nongate of the GAIM part were of much severer deformation than that at the gate end. In contrast with GAIM moldings, the morphology at the gate end of the CIM moldings was in a greater deformation than that at the nongate end.

References

1. Stevens, T. Mater Eng 1991, 108, 28.
2. Kirkland, C. Plast World 1991, 49, 37.
3. Chen, S. C.; Hsu, K. S.; Hung, J. S. Ind Eng Chem Res 1995, 34, 416.
4. Chen, S. C.; Hsu, K. F.; Hsu, K. S. J Appl Polym Sci 1995, 58, 793.
5. Turng, L. S.; Wang, V. W. SPE ANTEC Tech Pap 1991, 37, 297.
6. Chen, S. C.; Cheng, N. T.; Sheng, H. K. Int J Mech Sci 1996, 38, 335.
7. Chen, S. C.; Cheng, N. T.; Hsu, K. S. Int Commun Heat Mass Transfer 1995, 22, 319.
8. Chen, S. C.; Cheng, N. T. Int Commun Heat Mass Transfer 1996, 23, 215.
9. Clark, C. L.; Williarns, R.; Jeffrey, S.; Bi, S. Plast Eng 1996, 52, 35.
10. Chien, R. D.; Chen, S. C.; Chen, Y. C. Plast Rubber Compos 2002, 31, 336.
11. Khayat, R. E.; Derdouri, A.; Hebert, L. P. J Non-Newtonian Fluid Mech 1995, 22, 253.
12. Turng, L. S. Process Eng Plast 1995, 8, 171.
13. Rothe, J. Kunstst Ger Plast 1988, 78, 19.
14. Li, C. T. Polym Eng Sci 2004, 44, 992.
15. Zhou, H. M. Poly Eng Sci 2003, 42, 91.
16. Chen, S. C.; Cheng, N. T. Int J Heat Mass Transfer 1996, 23, 215.
17. Chen, S. C.; Dong, J. G.; Jong, W. R.; Huang, J. S.; Jeng, M. C. SPE Tech Papers 1996, 43, 663.
18. Chien, R. D.; Chen, S. C.; Kang, Y.; Yeh, H. Y. J Reinf Plast Compos 1998, 17, 1213.
19. Grelle, P. F.; Kallman, M. A.; Tallmadge, B. J. Presented at the SPI Structural Plastics Conference and Parts Competition, Washington, April, 1994.
20. Hu, S. Y.; Chien, R. D.; Chen, S. C.; Kang, Y. Plast Rubber Compos Process Appl 1996, 26, 172.
21. Chien, R. D.; Chen, S. C.; Jeng, M. C.; Yang, H. Y. Polymer 1999, 40, 2949.
22. Liu, S. J.; Chen, Y. S. Compos Appl Sci Manuf 2004, 35, 177.
23. Melaughlin, K. W. Polym Eng Sci 1989, 29, 1560.
24. Hsiung, C. M.; Cakmak, M.; Ulcer, Y. Polymer 1996, 37, 4555.
25. Ohlsson, B.; Tonell, B. Polym Eng Sci 1998, 38, 108.
26. Son, Y.; Ahn, K. H.; Char, K. Polym Eng Sci 2000, 40, 1385.
27. Tadmor, Z. J Appl Polym Sci 1974, 18, 1753.
28. Tan, V.; Kamal, M. R. J Appl Polym Sci 1978, 22, 2341.
29. Katti, S. S.; Schultz, J. M. Polym Eng Sci 1982, 22, 1001.
30. Fellahi, S.; Favis, B. D.; Fisa, B. Polymer 1996, 37, 2615.
31. Son, Y.;Ahn, K. H.; Char, K. Polym Eng Sci 2000, 40, 1376.
32. Li, Z. M.; Yang, W.; Yang, S. Y.; Huang, R.; Yang, M. B. J Mater Sci 2004, 39, 413.
33. Lee, M. P.; Hiltner, A.; Baer, E. Polymer 1992, 33, 685.
34. Reid, R. C.; Prausnitz, J. M.; Poling, B. E., The Properties of Gases and Liquids, 4th ed., New York: Mc Graw Hill, 1987; p 738.
35. Wang, D. Y.; Wang, J.; Qu, X. Z.; Liang, R. F., Qi, Z. N. Acta Polym Sinica 2000, 44, 11.
36. Lee, M. P.; Hiltner, A.; Baer, E. Polymer 1992, 33, 675.